Available online at www.sciencedirect.com
SCIENCE DIRECT®
Pergamon
Cement and Concrete Research 34 (2004) 391–397
CEMENT AND CONCRETE RESEARCH

Experimental study on AE characteristics of three-point-bending concrete beams

Bing Chen[a,*], Juanyu Liu[b]

[a]School of Civil Engineering and Mechanics, Shanghai Jiaotong University, Shanghai 200240, PR China
[b]Department of Civil Engineering, Texas A&M University, College Station, TX 77843, USA

Received 18 March 2003; accepted 18 August 2003

Abstract

In this research, acoustic emission (AE) characteristics of three-point-bending concrete beams were investigated during the entire loading period. It was found that the relative notch depth significantly influenced AE characteristics. The occurrence of AE events decreased greatly with an increase of the relative notch depth. The influences of different fibers in concrete on AE characteristics were investigated as well. The experimental results indicated that the Weibull function can be used to describe quantitatively the influences of the relative notch depth and fibers on AE characteristics, fracture characteristics, and brittleness of concrete. The two parameters, θ and m, of the Weibull function depended on the geometry of the concrete specimens and the brittleness of concrete, respectively.

Keywords: Acoustic emission, (AE); Concrete; Microcracking; Brittleness

1. Introduction

Acoustic emission (AE) is a kind of microseismic wave generated from dislocations, microcracking, and other irreversible changes in a stressed material. The monitoring of stress waves is accomplished by piezoelectric transducers, which convert these mechanical waves to electrical signals.

The AE technique is a widely used tool for nondestructive evaluation of metallic and nonmetallic materials and engineering structures [1–4]. It differs from most other nondestructive methods in two significant aspects [5]. First, the energy detected is released from the interior of the tested object rather than from some external sources. Second, AE techniques are capable of detecting the dynamic processes associated with the degradation of structural integrity. Recently, the AE technique has also been applied to studies of concrete mechanics, with a focus on the properties of crack extension during the fracture process [6–8].

In the research on fracture toughness of concrete [9–12], a three-point-bending concrete beam with a single notch is a typical specimen used model concrete fracture mechanics whose relative notch depth has significant effects on the brittleness and fracture properties of the specimen [13].

In order to investigate the sources of brittleness of concrete, AE characteristics of three-point-bending concrete beams with and without different fibers were investigated in this study, and the effects of the relative notch depth and intrinsic properties of concrete specimens on the brittleness of concrete were studied as well.

2. Experimental details

2.1. Sample preparation

Two series of concrete beams were prepared for this study: (1) normal concrete beams with different notch depths and the same mix proportions; and (2) concrete beams containing different fibers at the notch depth of 50.0 mm. The details of the mix proportions are listed in

* Corresponding author. Tel.: +86-21-5474-4095; fax: +86-21-5474-4255.
E-mail address: hntchen@sjtu.edu.cn (B. Chen).

0008-8846/$ – see front matter © 2004 Elsevier Ltd. All rights reserved.
doi:10.1016/j.cemconres.2003.08.021

Table 1
Mix proportion

Series	Water, kg/m^3	Cement, kg/m^3	Slag, kg/m^3	Sand, kg/m^3	Gravel, kg/m^3	Fiber, kg/m^3
Normal concrete	168	267	115	740	1110	/
Steel fiber concrete	168	267	115	740	1110	70
PP fiber concrete	168	267	115	740	1110	2

Table 1. The specimens were demolded 1 day after casting and then were cured in a curing chamber at 17–23 °C and a relative humidity greater than 90%. Two days before testing, they were taken out for single edge notch cutting according to the requirements of the experiments.

2.2. Testing equipments

Three-point-bending tests were performed using an Instron 8501 Digital Servo hydraulic testing system. The specimen dimensions were 100 × 100 × 515 mm, with single edge notch at depths of 20.0, 50.0, or 80.0 mm, as shown in Fig. 1. Six PACR15 transducers with a resonant frequency of approximately 150 kHz were glued onto the two opposite surfaces of the specimens to monitor the AE activities. The deflections at the midspan of beams were also measured.

A SPARTAN-AT2000 AE system was used for AE data acquisition. The AE signals were amplified with a gain of 40 dB in a preamplifier and a gain of 20 dB in the system. A threshold of 40 dB was selected to ensure a high signal-to-noise ratio.

3. Experimental results

3.1. Effect of relative notch depth on AE characteristic

The correlations between AE events and the $P-\delta$ curves of concrete beams with different relative notch depths are shown in Fig. 2. It was found that the occurrence of AE had a good correlation with the load versus the deflection curve. In the ascending branch of the $P-\delta$ curves, the AE characteristics of concrete beams with different relative notch depths were similar: (1) During the initial loading stage, there was little occurrence of AE activities; (2) As the load reached about 80% of the failure load, the AE activity became more intense; (3) When the external load exceeded the ultimate strength, the AE activity increased rapidly. In the descending branch of the $P-\delta$ curves, the relative notch depth had a great effect on AE characteristics: (1) The position of the peak of occurring AE events changed with the relative notch depth. The peak appeared in the region of 85–95% of ultimate strength on the descending branch of the $P-\delta$ curves when the relative notch depth was 0.2, while it appeared in the region of 60–80% P_{max} in the descending branch of the $P-\delta$ curves when the relative notch depth was 0.5. However, there did not exist an AE peak during the entire loading processes when the relative notch depth was 0.8. (2) The width of the occurring AE events peak increased with an increase of the relative notch depth. Therefore, the position of the peak shifted to the latter part of the descending branch of the $P-\delta$ curves, the width of the peak increased, and the magnitude of the peak decreased with an increase of the relative notch depth. As the relative notch depth became larger, no peak occurred, which indicated that the occurrence of AE decreased with an increase of the relative notch depth; this is the brittleness of the specimen decreased.

3.2. Effect of fibers on AE characteristic

The effects of fibers on AE characteristics during the entire loading processes are shown in Fig. 3. From the $P-\delta$ curves, it can be seen that there existed a plateau at the maximum load for the fiber reinforced concrete, which indicated that fibers decreased the brittleness of the concrete beams. Accordingly, AE characteristics showed the similar trends: the distribution of occurring AE events for normal concrete peaked in the region of 80–90% of the maximum load in the descending branch of the $P-\delta$ curve, while that for fiber reinforced concrete was scattered, with no obvious occurring AE event peak.

3.3. Correlation between AE events and fracture processes

A typical experimental record for the $P-\delta$ and $dN/dt-\delta$ curves is shown in Fig. 4. It was found that the relationship between dN/dt and δ could be divided into three stages: (1) $dN/dt=0$ (i.e., there was no AE); (2) the relationship between dN/dt and δ was discontinuous; and

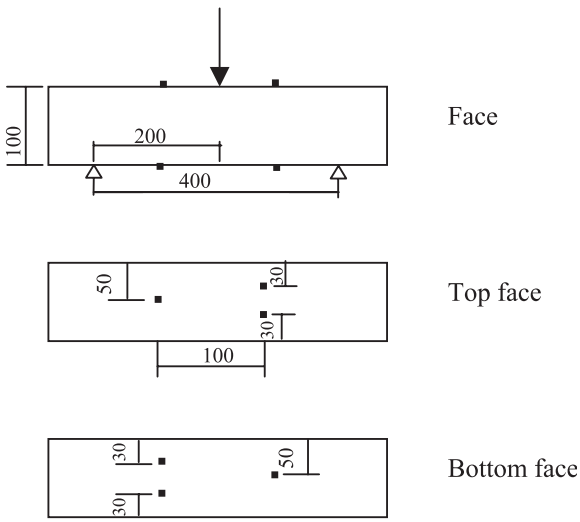

Fig. 1. Geometry of specimen and position of transducers.

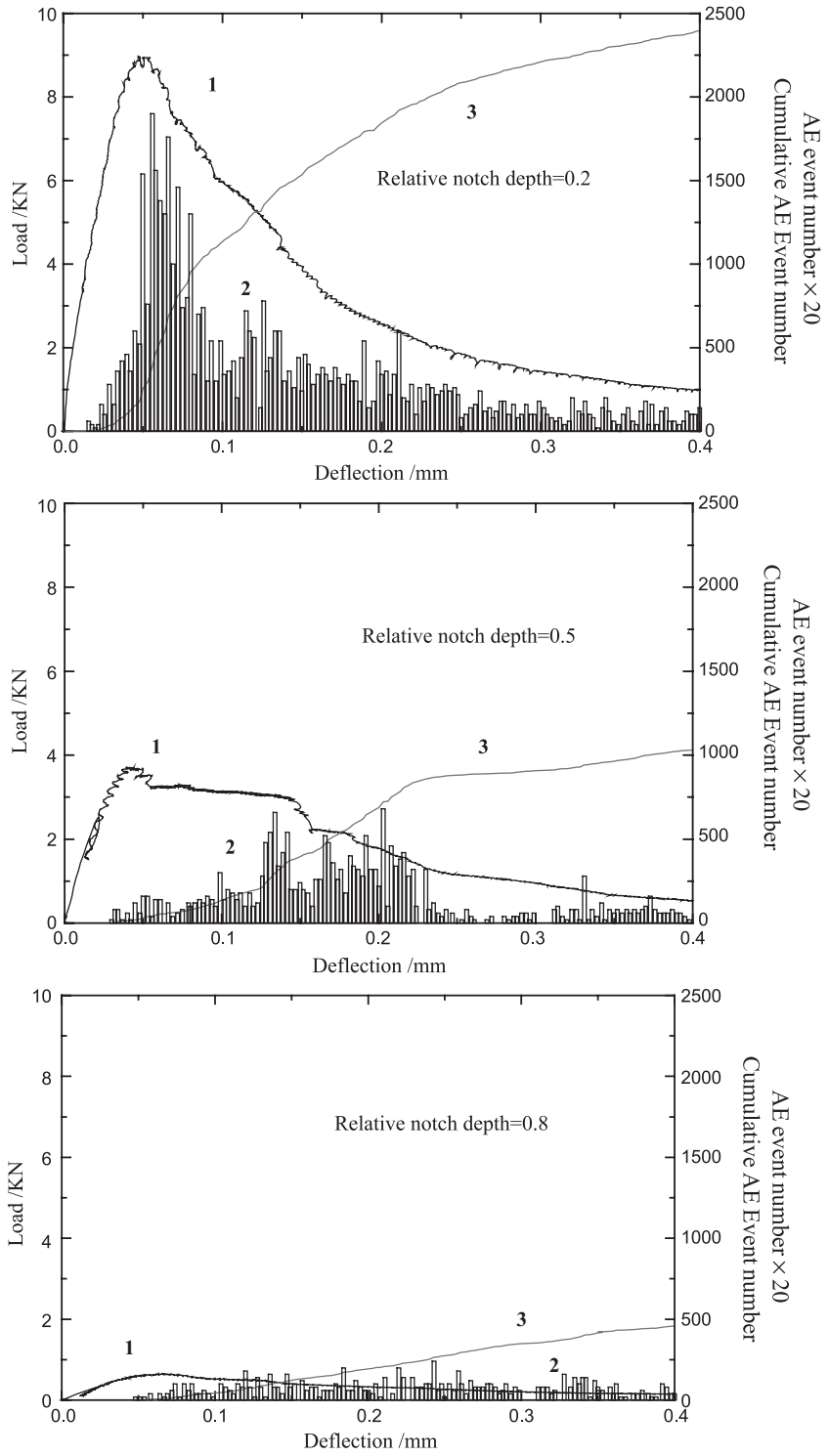

Fig. 2. AE characteristic for concrete beams with different relative notch depth; 1—load, 2—AE event rate, 3—cumulative AE event number.

(3) the relationship between dN/dt and δ was continuous. From further analysis of $dN/dt-\delta$ curves, it can be considered that the fracture process of three-point-bending beams consisted of three stages: stable microcracking, coalescence of microflaws and growth of the microcracks, and connection of the main cracks.

(1) Stable microcracking: when the load was less than the maximum load, microflaws in the interior of the concrete could not extend and they were in a stable state.
(2) Coalescence of microflaws and growth of microcracks: when the load reached the maximum load (which

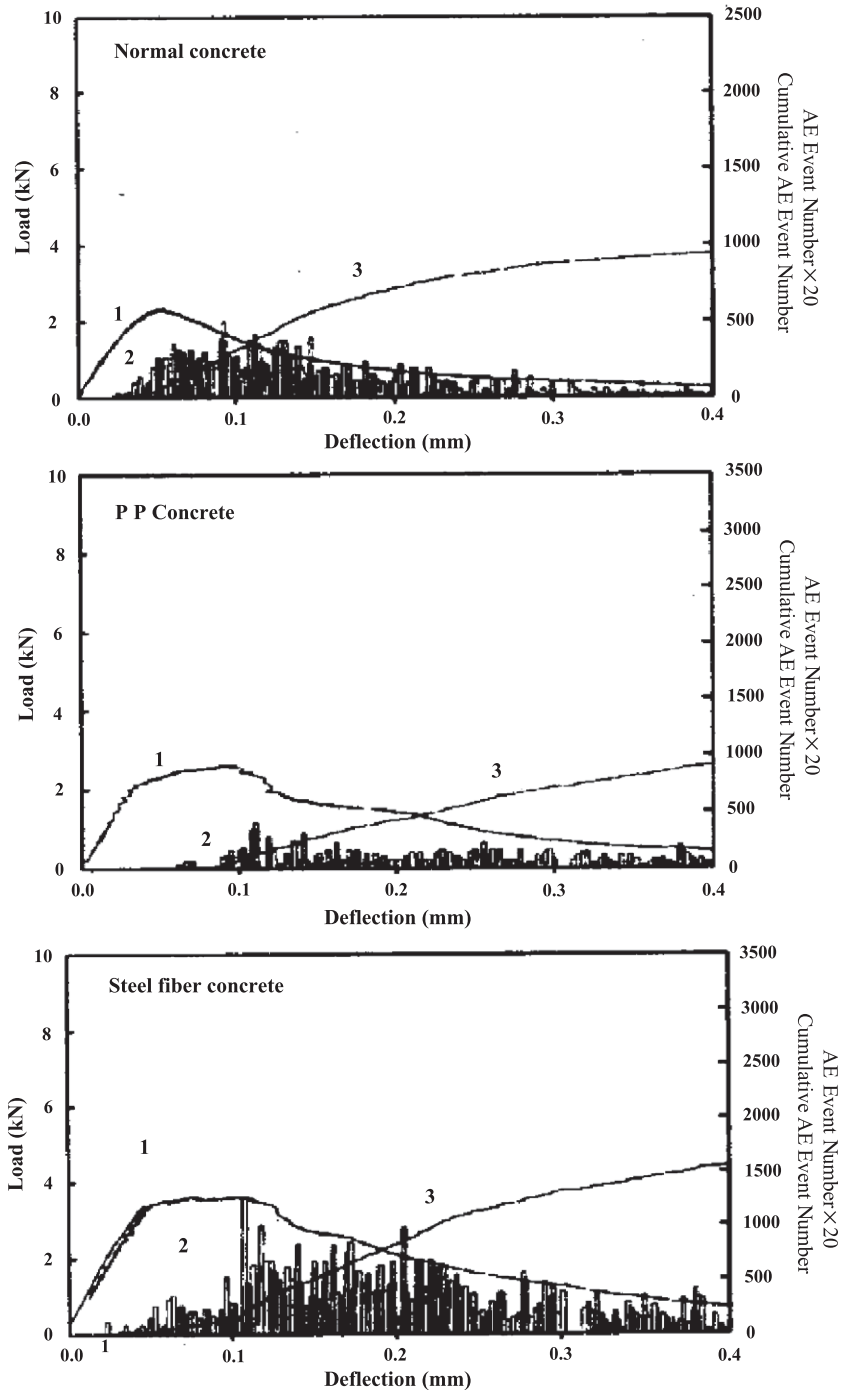

Fig. 3. AE characteristic for concrete beams with different fibers; 1—load, 2—AE event rate, 3—cumulative AE event number.

means the deflections beyond the deflection at peak load), the microcracks around the tip of the main cracks began to grow while the main cracks themselves did not extend. Hence, the relationship between dN/dt and δ was discontinuous.

(3) Growth of main cracks: When the external load reached to the critical load, the main cracks began to grow. Thus, the relationship between dN/dt and δ was continuous.

Therefore, the trend of occurring AE events corresponds to the microfracture processes of concrete in three-point-bending.

4. Analysis and discussion

According to the statistical theory of damage of quasi-brittle materials, concrete can be considered to be composed

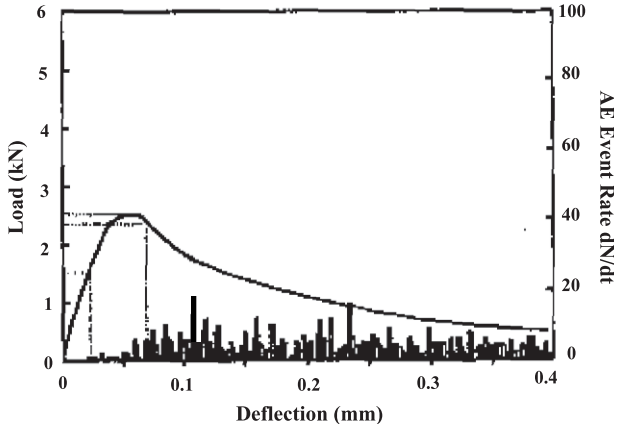

Fig. 4. Typical $P-\delta$ curve and $dN/dt-\delta$ curve from experiment.

of many microelements. Under the external load, the rupture probability of each microelement is different but normally complies with a Weibull distribution. For instance, some research has shown that under uniform uniaxial tensile strain, the rupture probability density function of the microelement could be described as follows:

$$f(\varepsilon) = \theta m(\varepsilon - \varepsilon_0)^{m-1}\exp[-\theta(\varepsilon - \varepsilon_0)^m] \quad (1)$$

where θ and m are parameters related to the size and deformation properties of the specimen, respectively. ε_0 is a constant determined by experiments.

When the strain reaches a certain value, the rupture probability of the microelement occurring in the material becomes:

$$F(\varepsilon) = \int_0^{\varepsilon} f(\varepsilon) = 1 - \exp[-\theta(\varepsilon - \varepsilon_0)^m] \quad (2)$$

Although the rupture condition of three-point-bend beams is much more complicated than that of the specimens under uniaxial tensile loading and the distribution of strain is not uniform, it is still reasonable to consider that each AE event is the result of the rupture of a microelement. Therefore, the rupture probability density of the microelements in concrete at a time (corresponding to a certain deflection) can be presented by the ratio of the AE hit ratio ($dN/d\delta$) to the total number of AE hits (N_{tot}), i.e.,

$$f(\delta) = \frac{dN_\delta}{d\delta} \Big/ N_{\text{tot}} \quad (3)$$

While the rupture probability of the microelement at that time is:

$$F(\delta) = N_\delta / N_{\text{tot}} \quad (4)$$

From the fit of the experimental data, it was found that the Weibull function was perfectly suitable for describing the statistical distribution characteristics of AE events and the rupture probability of the microelement for three-point-bending concrete materials, with a correlation (average of nine specimens) of 99.5%. As an example, Fig. 5 shows the coincidences between the Weibull function and AE hit ratio curves of three-point bending beams with three different relative notch depths. In Fig. 5, the points represent the experimental data, while the straight line was the result of bilogarithmic fitting of AE cumulation obtained from the experiments. The correlation between Weibull function integration curves and the measured AE hit ratio–deflection curves is shown at the top left of the figure, while the correlation between Weibull function integration curves and tested AE cumulation curves is shown at the bottom right of the figure. Therefore, the rupture probability density and the rupture probability ratio of the microelement for three-point-bending concrete beams can be described by the Weibull function, namely,

$$f(\delta) = (dN_\delta/d\delta)/N_{\text{tot}} = \theta m(\delta - \delta_0)^{m-1}\exp[-\theta(\delta - \delta_0)^m] \quad (5)$$

$$F(\delta) = N_\delta/N_{\text{tot}} = 1 - \exp[-\theta(\delta - \delta_0)^m] \quad (6)$$

The values of m, θ, and fracture energy G_f for concrete beams with different relative notch depths are shown in Table 2. For these concrete beams, the components of concrete were the same while the dimensions of the specimens were different. It was found that the value of m did not change with a change of the relative notch depth, while the values of θ and G_f decreased greatly with increasing relative notch depths. Table 3 gives the values of m, θ, and fracture energy G_f for concrete beams with different fibers. For these concrete beams, the dimensions of the specimens were the same and the components different. In this case, the values of m and G_f changed greatly for concrete beams containing different fibers, while the value of θ was almost unchanged. In addition, the values of m and G_f were the least for normal concretes and the largest for concretes with steel fibers.

The fracture properties and brittleness of concrete come from two aspects: one is from the intrinsic brittleness of the material, the other is from the geometric properties of the specimen. According to the experimental results, the two parameters, θ and m, in the Weibull function depend on the geometry of the concrete specimens and the brittleness of the concrete, respectively. Therefore, the brittleness of concrete beams can be determined quantitatively by AE techniques during the entire loading process.

5. Conclusions

(1) The failure processes of three-point-bending concrete beams with different relative notch depths and same specimen dimensions have different AE characteristics.

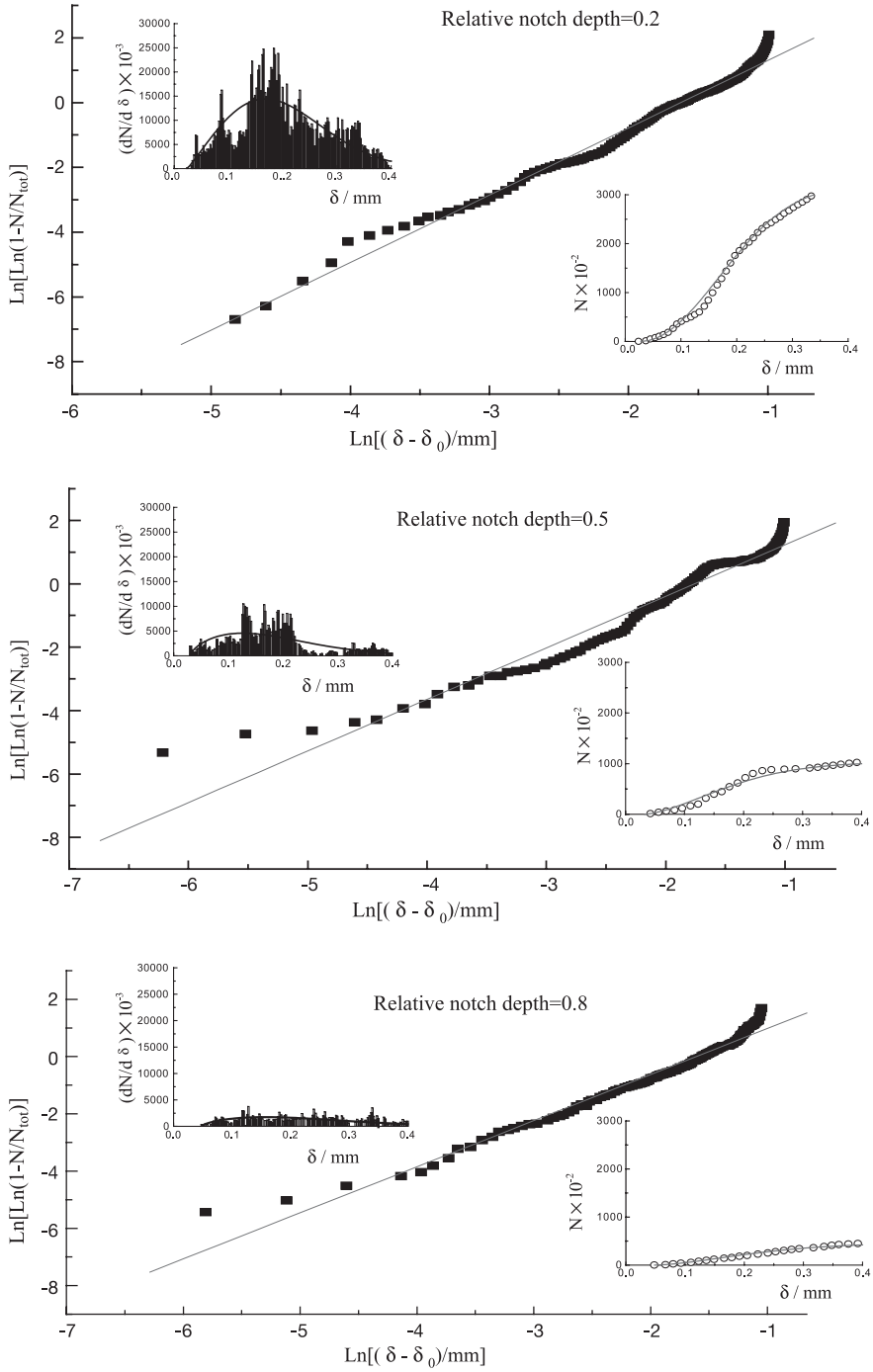

Fig. 5. The fitting curve of AE rate for concrete beams with different relative notch depth.

With the increase of the relative notch depth, the position of the peak of AE events shifts to the latter part of the descending branch of the corresponding $P-\delta$ curve. The width of the peak increases, the height of the peak decreases, and the occurrence of AE decrease as well.

Table 2
m, θ, δ_0, and G_f for normal concrete with different relative notch depth

Relative notch depth	θ	m	δ_0	G_f
0.2	24.93	1.83	0.02	255
0.5	19.35	1.60	0.033	160
0.8	14.1	1.74	0.04	90

Table 3
m, θ, δ_0, and G_f for concrete with different fibers

Series	θ	m	δ_0	G_f
Normal concrete	19.35	1.60	0.033	160
PP fiber concrete	19.58	1.86	0.04	184
Steel fiber concrete	19.63	2.04	0.024	315

(2) The statistical distribution characteristics of AE events of three-point-bending notched beams accord with the Weibull function, where θ represents specimen brittleness resulting from the geometry of the specimens, and m represents the intrinsic brittleness of the material. The greater the value of θ, the more brittle the specimen. The greater the value of m, the less brittle the material.

References

[1] A. Kumar, A.P. Gupta, Acoustic emission in fiber reinforced concrete, Exp. Mech. 36 (3) (1996) 258–261.
[2] A.K. Maji, R. Sahu, Acoustic emission from reinforced concrete, Exp. Mech. 34 (6) (1996) 379–387.
[3] H.L. Chen, C.T. Cheng, S.E. Chen, Determination of fracture parameters of mortar and concrete beams by using acoustic emission, Mater. Eval. (7) (1992) 888–893.
[4] K. Wu, B. Chen, W. Yao, Study of the influence of aggregate size distribution on mechanical properties of concrete by acoustic emission technique, Cem. Concr. Res. 31 (2001) 919–923.
[5] C. Ouyang, E. Landis, S.P. Shah, Damage assessment in concrete using quantitative acoustic emission, J. Eng. Mech. 117 (11) (1991) 2682–2690.
[6] J.M. Bethelot, J.L. Robert, Modeling concrete damage by acoustic emission, J. Acoust. Emiss. 6 (1) (1987) 43–60.
[7] M.K. Lim, T.K. Koo, Acoustic emission from reinforced concrete beams, Mag. Concr. Res. 41 (149) (1989) 229–234.
[8] H. Mihashi, N. Nomura, S. Niiseki, Influence of aggregate size on fracture process zone of concrete detected with three dimensional acoustic emission technique, Cem. Concr. Res. 21 (5) (1991) 737–744.
[9] P. Nallathambi, B.L. Karihaloo, Determination of specimen-size independent fracture toughness of plain concrete, Mag. Concr. Res. 38 (135) (1986) 69–76.
[10] G.V. Guinea, J. Planas, M. Elices, Measurement of the fracture energy using three-point bend tests: Part 1. Influence of experimental procedures, Mat. Struct. 25 (3) (1992) 212–218.
[11] M.F. Kaplan, Crack propagation and the fracture of concrete, J. Am. Concr. Inst. 58 (11) (1961) 591–610 (Proceeding).
[12] D.J. Naus, J.L. Lott, Fracture toughness of Portland cement concrete, J. Am. Concr. Inst. 66 (6) (1969) 481–489.
[13] V.E. Saouma, C.C. Barton, N.A. Gamaledin, Fractal characterization of fracture surface in concrete, Eng. Fract. Mech. 35 (1) (1990) 47–53.